THE JOURNAL OF PHYSICAL CHEMISTRY C

Article

pubs.acs.org/JPCC

Low Electric Field Intensity and Thermotropic Tuning Surface Plasmon Band Shift of Gold Island Film by Liquid Crystals

Jing Xie,[†] Xuemin Zhang,[†] Zenghui Peng,[‡] Zhanhua Wang,[†] Tieqiang Wang,[†] Shoujun Zhu,[†] Zhaoyi Wang,[†] Liang Zhang,[†] Junhu Zhang,*[,†] and Bai Yang[†]

[†]State Key Laboratory of Supramolecular Structure and Materials, College of Chemistry, Jilin University, Changchun 130012, People's Republic of China

[‡]State Key Laboratory of Applied Optics, Changchun Institute of Optics, Fine Mechanics and Physics, Chinese Academy of Sciences, Changchun, Jilin 130033, People's Republic of China

Supporting Information

ABSTRACT: By applying an electric field to nematic liquid crystals (LCs) to change the molecular alignment of LCs, we achieve feasible tuning of the localized surface plasmon resonance (LSPR) of novel gold island film immersed in the LCs, realizing the switching behavior of LSPR at low electric field intensity. In addition, we find that the liquid crystal can amplify the angle dependence of gold island film LSPR, which may provide a new method for research on the tiny and indistinct change of the gold nanoparticles' LSPR. At the same time, the LSPR can be used for detection of nematic LCs' thermal−optic effect, especially when the temperature is around the clearing point. For the entire experimental procedure, self-assembly and experimental tests are simple and require only common laboratory supplies and equipment, and both of them are novel relative to previous studies, which help us further investigate coupling the metal nanoparticles with the LCs.

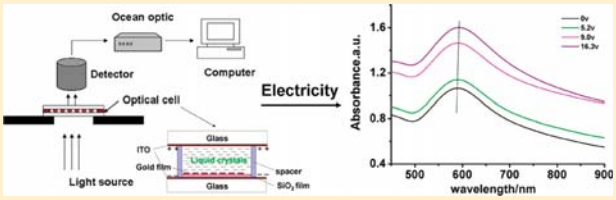

INTRODUCTION

Noble metal nanoparticles have attracted broad interest because of their intense tunable absorption and scattering resonance.[1] Centuries before, it has been known in Rome that reduction of noble metallic ions in the glass-forming process yields stained glass windows with ruby red color. While in the modern scientific system, this brilliant color is understood as incident photon frequency resonant with the collective oscillation of the conduction electrons for noble metal nanoparticles, known as localized surface plasmon resonance (LSPR).[2,3] Experimentally, LSPR is manifested as an obvious surface plasmon absorption band and an enhancement of the local electromagnetic field, which are sensitive to the size and shape of the nanostructures and the distance between them, as well as the effective refractive index (RI) of the local surrounding environment.[1,4,5] For Au and Ag nanoparticles, whose LSPR can be observed in the visible to near-IR part of the optical spectrum, they have applications in a variety of simple, well-developed setups of UV−vis transmission or reflection spectroscopy.[1,6,7] Moreover, chemical[7−11] and biological[12−20] sensing based on LSPR transducers are widely used.

Liquid crystals (LCs) have a large optical anisotropy due to their anisotropic molecular shape and alignment, and their alignments are extremely sensitive to external parameters such as light[21−24] and electric field.[25−29] As an outstanding medium example of an electro-optically active dielectric medium, it has major applications in displays,[30] optical periodical structures,[31,32] and color tunable polymer gratings.[33,34] Thus far, LC-based active tuning of metal nanostructures' LSPR has been demonstrated by an electro-optical mechanism, in which the phase transformation of the LCs through an electric field is controlled.[35−38] Meanwhile, the phase transition between the LC phase and the isotropic phase or between different kinds of phase can also induce changes in their optical properties.[39] It has also been reported that LCs may be useful for enhancing the sensitivity of LSPR-based detection of binding events and LSPR measurements of gold nanodots provide a means to characterize the nanoscopic origins of macroscopic, adsorbate-induced LC ordering transitions.[40]

Coupling metal nanoparticles with LCs has been widely studied in recent years.[41−45] Abbott et al. have coupled chemically functionalized gold nanoparticles with thermotropic LCs and have used LSPR or darkfield microscopy to track the local ordering of the LCs around the nanoparticle.[46−48] The Stark group,[49−51] the Terentjev group,[52−54] and the Yokoyama group[55−57] have reported a comprehensive and detailed mechanism on the surface of the LCs and the nanoparticles, as well as the interaction of the nanoparticles. We find that, in previous studies, it is accessible to achieve the electric control only when the electric field intensity is relatively high, even reaching a few hundred volts. Moreover, just alternating current is permitted to detect the experimental phenomenon.

In this paper, we represent a more simple and economical method to achieve the electric tuning of surface plasmon band

Received: October 12, 2011
Revised: December 22, 2011
Published: January 6, 2012

dx.doi.org/10.1021/jp2098312 | J. Phys. Chem. C 2012, 116, 2720−2727

shift of gold nanoparticle arrays by liquid crystals, in which the direct current power voltage is less than 30 V, making it possible to tune the optical resonances of noble metal nanoparticles at low electric field intensity. We also give detailed information about the cooperative nature of LC ordering transitions, which provides a means to amplify the LSPR responses of gold nanoparticles and LC's electro-induced phase transitions, as well as thermal tuning of LSPR in the optical cell.

EXPERIMENTAL SECTION

Overall, gold island film was constructed on the ITO substrate, with which the optical cell was prepared to detect the electro-optic effect of the liquid crystals (LCs). In our example, to facilitate the transformation of gold island from gold nanoparticle through thermal anneal, an interlayer of SiO_2 film was sandwiched between the gold island and the ITO substrate. Concretely, the SiO_2 film was prepared by spinning the SiO_2 precursor on the ITO coated glass, and the island film was prepared by horizontal lifting of gold nanoparticles to the SiO_2 substrate and subsequent high-temperature annealing. Experimental materials and concrete steps are as follows.

Materials. The gold island film was fabricated as follows. Indium tin oxide (ITO) coated glass slides (15 × 30 mm^2, 20 × 30 mm^2) used as substrates were cleaned by immersion in hot H_2O_2 for 20 min to create a hydrophilic surface followed by rinsing with quadruply distilled water four times in an ultrasonic bath (Cole-Parmer 8890) and drying under a steam of nitrogen. Other chemical reagents were all used without any purification.

Preparation of a SiO_2 Inorganic Film. The SiO_2 precursor was prepared according to Paul Mulvaney's sol−gel method.[58] The well-prepared SiO_2 precursor was diluted with ethanol, spun at different spin-coating rates for 1 min, heated at 135 °C to remove the water vapor, and then, calcined at high temperatures to make the SiO_2 nanoparticle inorganic. Subsequent O_2 plasma treatment could increase the hydrophilicity of the substrate's surface by producing more −OH so that the gold nanoparticle could be easily lifted to the ITO side. Wiping with absorbent cotton one-sided along the same direction before lifting the gold nanoparticle can cause micrometer thick films of nematic LCs to be anchored parallel to the surface.[59]

Building of an Island Film on a SiO_2/ITO Substrate. Aqueous gold sol with average diameters of 35 nm were prepared according to the method of Frens.[60] In brief, 2 mL of a 1% aqueous $HAuCl_4 \cdot 3H_2O$ solution was added to 198 mL of triply deionized water. After it was boiled, a 1 mL solution of 2% sodium citrate was added to the solution, boiled for 20 min, and then, cooled down to room temperature gradually with stirring. Then, 10 mL of the aqueous gold sol was transferred to a 30 × 30 × 60 mm^3 weighting bottle (for 20 × 30 mm^2 ITO glass, 15 mL of aqueous gold sol was transferred to a 40 × 25 × 25 mm^3 weighting bottle), and 1 mL of hexane was added to the top of the colloid solution surface to form an immiscible water/hexane interface. About 3.2 mL of absolute ethanol (for 15 mL of gold sol, the absolute ethanol was 3.6 mL) was then added dropwise to the hexane layer, which led to gold nanoparticles being trapped at the interface. By horizontal lifting of the gold monolayer from the water/hexane interface, 2D gold nanoparticle arrays on substrate were prepared.[61−63] Finally, an anneal treatment at 500 °C was carried out to make the gold nanoparticles coalesce and dewet on the substrate, rendering formation of the gold island film.

Infiltration of Liquid Crystals into the Optical Cell. The optical cell consisted of LCs sandwiched between a bare ITO-coated glass slide and an island film that was immobilized on an ITO-coated glass substrate. LCs were then infiltrated into the voids by using capillary forces at atmospheric pressure. Note that the LCs were heated above their phase transition temperature to convert them into the isotropic phase, enabling the voids to be filled fully. The schematic image of the optical cell structure is shown in Figure 1a.

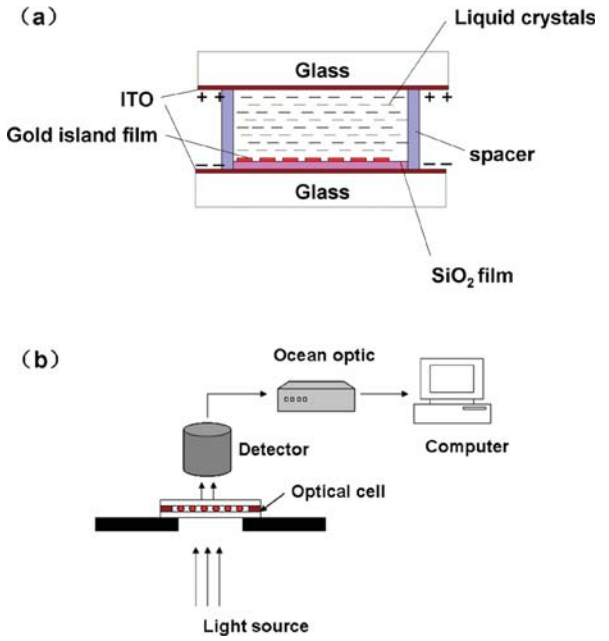

Figure 1. (a) Schematic image of the optical cell. (b) Experimental setup for electric field intensity and thermotropic tuning.

Characterization. Scanning electron microscopy (SEM) micrographs were taken with a JEOL JSM 6700F field emission scanning electron microscope with a primary electron energy of 3 kV. Atomic force microscopy (AFM) analyses were taken under tapping mode with a NanoscopeIII, a scanning probe microscope from Digital Instruments under ambient conditions. A Shimadu 3600 UV−vis−NIR spectrophotometer was used to measure SPB of the gold island film after heat treatment and the LSPR of the gold island film dependence on the surrounding environment's refractive index in the absorption mode. Electric and thermotropic tuning surface plasmon band shift of the gold island film were measured by Ocean Optics Maya Pro2000, the set up of which was illustrated in Figure 1b. The thicknesses of the SiO_2 films were determined using a Dektak150 surface profiler (Veeco). The refractive index (RI) of the LCs was determined using an Abbe refractometer.

RESULTS AND DISCUSSION

Detailed investigation of the morphology transformation of gold nanoparticle arrays and their optical properties as well as corresponding RIS (refractive index sensitivity) during the thermal treatment have been recently disclosed.[6] Generally, gold nanoparticles assembled on a substrate will experience a

dx.doi.org/10.1021/jp2098312 | J. Phys. Chem. C 2012, 116, 2720−2727

series process of melting, interparticle coalescence, and dewetting under thermal treatment, thus forming the so-called gold island film. Correspondingly, a blue shift trend with a concomitant of band narrowing of the surface plasmon band (SPB) is observed, which is due to the decreased coupling effect of adjacent gold island film compared with original gold nanoparticles. This process has been indicated helpfully for preparing LSPR based sensors because gold island film has a relative higher figure of merit. That is the essential reason why we make use of gold island film rather than gold nanoparticle arrays in our system. Moreover, the Au island film is controllable and reproducible and its extinction remains similar in mass repeated experiments, which is also the major reason we choose gold island film.

During the experimental process, we deposit a thin SiO_2 film on the ITO substrate in order that the SiO_2 film can separate the gold island film from the ITO substrate. We find that, when the gold island film is formed on the ITO glass substrate, the peak of LSPR is almost located at 600 nm with a broad full width at half-maximum (fwhm) different from the LSPR of the gold island film on the SiO_2 layer. Figure S1 of the Supporting Information illustrates the SEM image of the Au island film on ITO from which we can see that the interparticle distance and nanoparticle diameter are very different from that on SiO_2

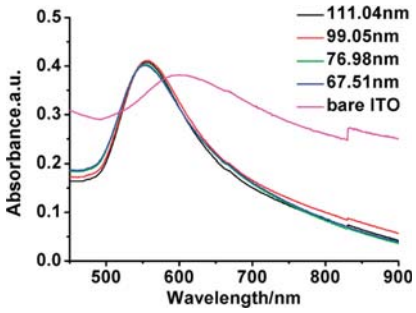

Figure 2. Absorption spectra of gold nanoparticles on different SiO_2 film thickness and on the ITO-coated glass.

(Figure 3c). This may be attributed to the thermal behavior of gold nanoparticles on two kinds of substrates not being totally the same and also to the difference in refraction index between substrates. As we all know, when the LSPR exhibits a narrower fwhm, it is more sensitive to the local dielectric environment, so a thin SiO_2 film on the ITO substrate is prepared in our study. By regulating the dilution ratio of SiO_2 gel and the spin-coating rate, we get film thickness ranging from 111 to 67.5 nm. Figure 2 is the absorbance spectra of the gold island film on ITO-coated glass and on ITO glass covered by SiO_2 film with different thickness. When the silica interlayer is introduced, it is evident that the SPB blue shifts to 550 nm with narrower fwhm compared with that on the ITO-coated glass substrate. It also affirms that the SiO_2 film is simply serving as the insulating layer to avoid the interaction between the gold island film and the ITO-coated glass substrate, whose thickness has no impact on the position of the LSPR. In our experiment, we fix 67.5 nm as the SiO_2 insulating layer thickness.

We emphasize the influence of different annealing temperatures on the nanoparticles. Inspection of Figure 3 reveals that, with temperature ranging from 300 to 500 °C, an apparent band narrowing takes place with a SPB shift to shorter wavelengths. The blue shift of peak position and band narrowing is attributed to the increase of interparticle distance, thus a weakening of coupling effect. From 300 to 400 °C, the interparticle distance changes from ∼112 nm to ∼113 nm, so the extinction spectra blue shifts slightly, while from 400 to 500 °C, the interparticle distance changes from ∼113 nm to ∼125 nm, and the extinction spectra blue shifts obviously. In addition, band narrowing is also resulted from the reshaping of the gold island film. It is noted that the gold island film obtained at higher annealing temperature will be much more isotropic in shape than that obtained at lower annealing temperature, rendering SPB with a narrower fwhm. In our following experiment, because the extinction of the island film at 500 °C has a higher figure of merit, we all use 500 °C as the annealing temperature after the gold nanoparticles are horizontal lifted onto a substrate.

The wavelength of the peak absorption is known to be dependent on the dielectric environment of the nanoparticle.[1,5] An increase in the refractive index of the medium surrounding the nanoparticle results in a red shift in the wavelength of the absorption maximum.[4,46] Bulk RIS of obtained gold island film is measured by simply dipping the sample in air, water, chloroform, or carbon bisulfide, whose refractive indices are 1.00, 1.33, 1.45, and 1.63, respectively. Through the experiment, we can get the red-shifted SPB with the increase of refractive index (Figure 4), confirming the island film we have prepared possesses good tuning shift of LSPR when the refractive index surrounding changes. By a linear dependent fitting,[64,65] the RIS is determined at 89 nm per refractive index unit (RIU), in agreement with the analytical model.[66]

The ordering of the liquid crystal in the vicinity of the supported island film is very complex, requiring detailed description of the local dielectric environment, including the competing effects of the nanoparticles, glass surfaces on the ordering of the liquid crystal, and an account of the influence of topological defects about the nanoparticles.[67] In this paper, by introducing a SiO_2 film between the ITO layer and the island film, we consider a highly simplified model of the dielectric environment created by the liquid crystal near the surfaces of the island film. We record the extinction spectra before and after we embed the island film in the TEB-300 (one type of liquid crystal, $n_0 = 1.51$, $n_e = 1.67$, the clearing point is 64.6 °C, from Chengzhi Yonghua Display Materia Co., Ltd.). The datas are recorded under normal incidence of the probe light. When measured in air, the island film exhibits a peak of 550 nm (Figure 5, the black curve) in its optical extinction spectra. When the island film is embedded in LCs, it leads to a red shift in the LSPR peak of 41 nm (from 550 to 591 nm, the red curve). According to the RIS measured above, the theoretical shift of the peak wavelength is 45 nm, so the experimental value accords with the theoretical value in the systematic offset. Moreover, the measured refractive index of TEB-300 at room temperature is 1.514, corresponding to n_0 of TEB-300; hence, we get a conclusion that most LC molecules are parallel oriented to the substrate, which will be discussed later.

By measuring the spectrum at various angles of light incidence with unpolarized light, the plasmon reflectance peaks of the gold island film are revealed. Reflectance spectra are chosen as the test of the gold island film's angular dependence, because it is more convenient than other testing methods. Figure 6a, b are reflectance spectra of a gold island film on an ITO glass substrate and in a liquid crystal cell at various angles of light incidence, respectively. The LSPR of the gold island film in the optical cell represents a reflectance peak

dx.doi.org/10.1021/jp2098312 | J. Phys. Chem. C 2012, 116, 2720–2727

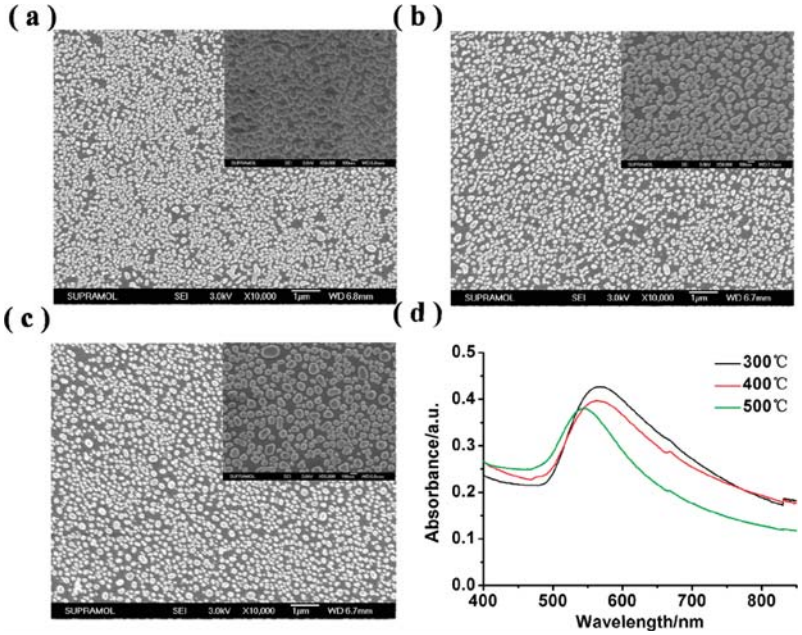

Figure 3. SEM images of the gold nanoparticle monolayer with calcining heat of (a) 300 °C, (b) 400 °C, and (c) 500 °C. (The insets are cross-sectional SEM images at 45° to the substrate normal, respectively.) (d) Absorption spectra of the gold nanoparticle monolayer at different temperatures.

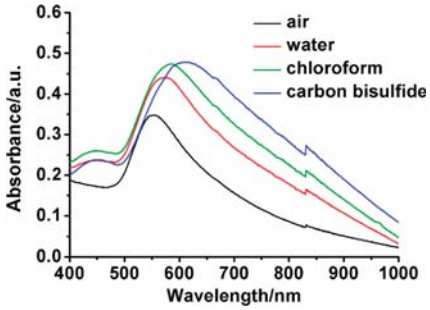

Figure 4. LSPR responses of gold island film to different solvents of air, water, chloroform, and carbon bisulfide.

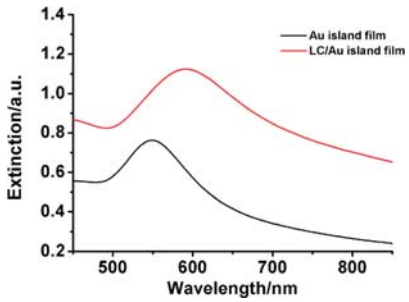

Figure 5. Extinction spectra of the gold island film before (the black curve) and after (the red curve) immersed in liquid crystals.

of 645.43 nm (in accordance with apparent red color), showing a red shift of the LSPR compared with the LSPR measured in air. When the beam was incident normal to the substrate, both the island film in air and the island film embedded in the LCs exhibit a single reflectance band (which is indicative of in-plane dipole resonance). As incident angle increases, the reflectance-LSPR (R-LSPR) shifts to a shorter wavelength with slight band broadening. From previous reports, it is known that, when gold naoparticles are tilted, other than in-plane resonance, the out-of-plane resonance plasmon is exited as well and the amount of light coupled to the normal plasmon and lateral modes is mostly governed by the light incidence angle.[36] Atomic force micrograph and SEM helps us further investigate the mechanism of the reflective spectra. They reveal that the gold island film used in our experiments has an average height of 73 nm and a lateral dimension of 100 nm. Compared with in-plane dipole resonance, the out-of-plane extinction band appears at the shorter wavelength due to relative small size. These two resonance overlap with each other and become indistinguishable for a gold nanoparticle with an aspect ratio $r \approx 1$. Consequently, in our experiment, the R-LSPR extinction band shows a blue-shift trend with a concomitant of band broadening as the tilt angle increases. Besides, it is worth noting that the angular dependent property of gold island film is amplified by introducing LCs as surrounding medium. We can clearly see that, when the gold island film is on an ITO glass substrate, the reflectance-LSPR (R-LSPR) gets a blue shift of 7.0 nm (from 576.14 to 569.14 nm) as the incident angle changes from 0° to 45°, while in the optical cell, the R-LSPR gets a blue shift of 16.76 nm (from 645.43 to 628.67 nm). We attribute this phenomenon to the birefringence of liquid crystal. When the incident light radiates on the LCs, the birefringence of liquid crystal will lead the deflection of the light along the direction of the director *n*, resulting in the increase of the out-of-plane resonance plasmon; therefore, the indistinguishable reflective spectra can be observed in the shorter wavelength compared with the gold island film in air. It is suggested that liquid crystal can amplify the angle dependence phenomenon of gold nanoparticles' LSPR; this may provide a new method for the research on the tiny and indistinct change of the gold nanoparticles' LSPR.

To establish the correlation between the peak shift of the LSPR and the electric field-induced phase transition in the

dx.doi.org/10.1021/jp2098312 | J. Phys. Chem. C 2012, 116, 2720–2727

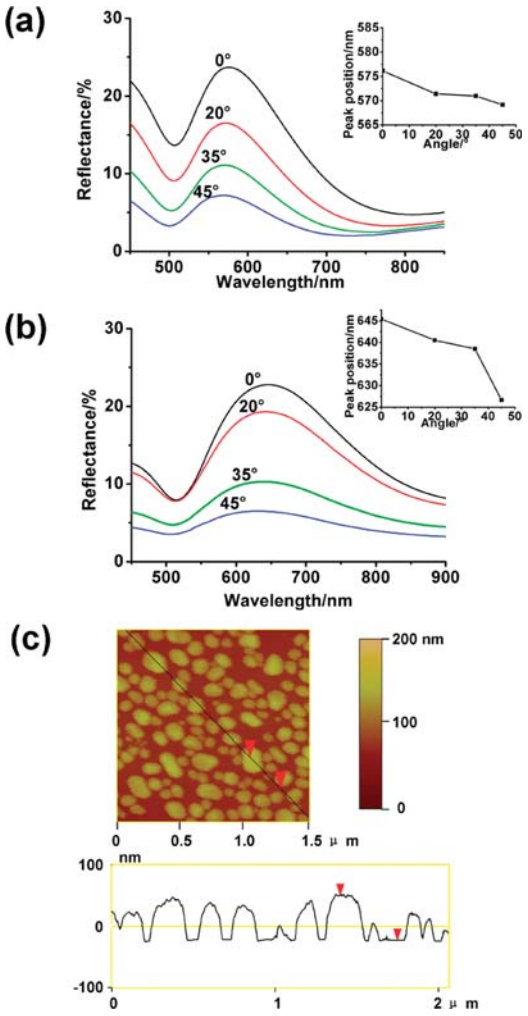

Figure 6. Angular dependence of the gold nanoparticles. (a,b) Reflectance spectra of nanoarrays at various angles of incidence measured in air and in liquid crystals (TEB-300), respectively. The insets in (a) and (b) show the peak position results of different incident angle. (c) AFM image and line profile of morphology evolution for two-dimensional gold nanoparticles with average diameters of 35 nm after 500 °C annealing.

electroresponsive LCs, control experiments are designed as follows. First, we wipe the ITO-coated glass slide so that the long axis of liquid crystal molecules can be parallel to the orientation of the substrate surface.[59] LC cells are fabricated, consisting of a bare ITO-coated glass slide and a gold island film that is immobilized on an ITO-coated glass substrate, with a thickness of 92 μm insulating films placed between the ITO-coated glasses to avoid a short circuit. After the optical cell is well-prepared, we connect it to the direct current power supply, and the datas are recorded under normal incidence of the probe light. Ocean optic Maya Pro2000 is used to detect the LSPR of the gold island film. The absorbance is low on the whole range because the light is scattering in the initial state, with a peak appeared at around 590 nm when no electric field is applied, which can be seen from Figure 7a. By manually changing the input voltage to the optical cell, changes in optical properties are measured during the application of different electric field intensities on the optical cell. With the increased voltage, the intensity of the LSPR increases, and the peak shifts toward longer wavelength. The increased absorbance arises from the decreased light scattered by LCs. Meanwhile, liquid crystal molecular orientation is better aligned parallel to the electric field so that the ratio of the molecules that align parallel to light propagation decrease. As a result, the component of the refractive index n_e for extraordinary light increases, and the averaged refractive index of the LC increases;[68] consequently, the peak shifts toward longer wavelength. Figure 7b is the electric field intensity dependence of the LSPR peak of the gold island film. The measurements are performed with the island film immersed in TEB-300.

In order to further investigate the electric-induced peak shift of LSPR by electro-optic effect of the nematic liquid crystal, another type of liquid crystal, SLC-9023 (Chengzhi Yonghua Display Materia Co.,Ltd.), is used, whose refractive index difference is 0.18 and the clearing point is 124 °C. Using the same experimental procedure as described previously, from the extinction spectra, we can see that the peak of the LSPR gets a red shift with the voltage increase (Figure 7c, d), the same as the experimental phenomena of TEB-300. These results show the tuning behavior of optical resonances of noble metal nanoparticle at low electric field intensity and the optical cell we have prepared can be well used to investigate the electro-optic effect of the nematic liquid crystal.

Furthermore, the reusing ability of LCs and chemical stability of the optical cell are measured. With increased voltage, the LSPR peak of the gold island film shifts to longer wavelength, and when the electric field is turned off, the peak of the LSPR returns to the original peak position. From Figure 8, we can see that cycling of the electric field intensity between 0 and 8 V results in reproducible changes in the positions of the maximum absorbance, affirming the LCs possess reversible electrical responsiveness and the optical cell we have prepared has good stability.

In the following experiment, positions and intensity of the LSPR peaks of the gold island film as a function of temperature are investigated (Figure 9). We clearly know that the temperature dependence of the local order of the liquid crystal near the nanoparticles is substantially different from bulk liquid crystal.[46] We fix the device on the heating plate with normal incidence light and gradually increase the temperature and simultaneously record the reflectance peak during the process. Inspection of Figure 9a reveals a significant decrease in the LSPR peak intensity with the increase of temperature, accompanied with negligible wavelength peak shift. This can be attributed to the bulk nematic-to-isotropic phase transition. At room temperature, the LCs are in nematic phase, from the macro point of view it performs white with high-viscosity liquid, accompanied with low scatter and high extinction. As the temperature increases, the ratio of the LC molecular in nematic phase decreases, resulting in the decreased extinction peak. When the temperature is higher than the clear point, the LCs are in anisotropic phase, and the extinction does not change any more. Figure 9b is the curve dependence of the intensity of the absorption peak as a function of temperature. By a linear fitting, we could get the breaking point at the 60.4 °C. In theory, when the temperature is at the vicinity of the clear point, a large number of LC molecules translate into anisotropic extinction, which would result in the rapid decrease in peak intensity, reflected in the peak-temperature curve as the breaking point. The breaking point of the experiment has deviation with the clear point but within the systematic offset, so we can get the conclusion that, by our method, the clear

dx.doi.org/10.1021/jp2098312 | J. Phys. Chem. C 2012, 116, 2720–2727

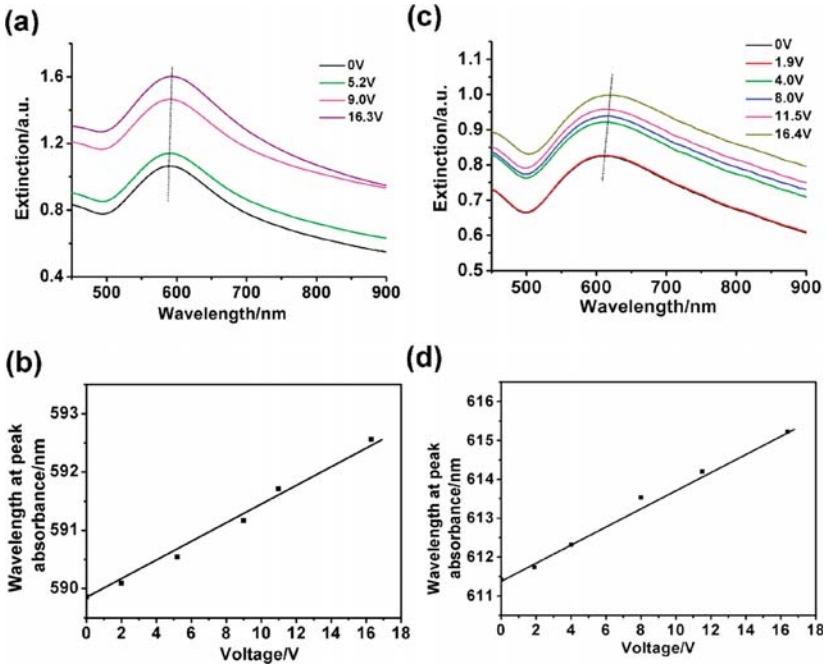

Figure 7. (a) Experimental extinction spectra at different electric fields measured in TEB-300. (b) Position of absorption peak as a function of electric field strength in TEB-300. (c) Experimental extinction spectra at different electric fields measured in SLC-9023. (d) Position of absorption peak as a function of electric field strength in SLC-9023.

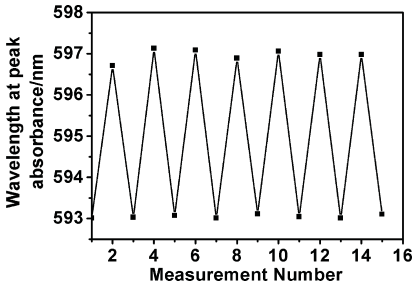

Figure 8. Reproducible changes of the wavelength peak of the LSPR as the electric field intensity is cycled from 0 to 8 V.

point of an unknown LC or the mixture can be intuitively predicted by the LSPR peak, which provides a new way to the research on the LCs.

■ CONCLUSIONS

In summary, a gold island film on ITO-coated glass is prepared, and morphology and optical properties of gold nanoparticle arrays are studied. Through the experiment, we find that the liquid crystal can amplify the angle dependence phenomenon of gold island film's LSPR, which may provide a new method for the research on the tiny and indistinct change of the gold nanoparticles' LSPR, and at the same time the LSPR can be used for the detection of LCs' electro-optic effect, especially realizing the switching behavior of LSPR when the electric field intensity is very low. For the thermal response of liquid crystals, we find an intuitionistic way to sense the LCs' temperature dependence by the LSPR shift of gold island film. Unlike other methods, self-assembly and experimental tests are simple and require only common laboratory supplies and equipment for the entire preparation process; thus, it maybe provide an effective and economic way to further research on noble metal nanoparticles' LSPR and electro-optic and thermal-optic effects of liquid crystals.

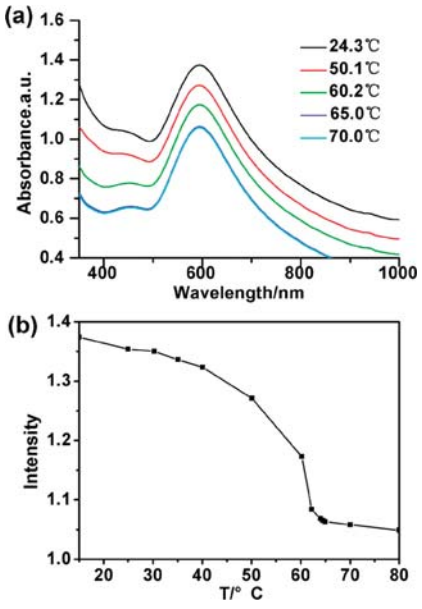

Figure 9. (a) Temperature dependence of the LSPR peak of gold nanoparticles immersed in TEB300. (b) Dependence of the intensity of absorption peak as a function of temperature.

■ ASSOCIATED CONTENT

Supporting Information

Figure showing SEM image of the Au island film on ITO. This material is available free of charge via the Internet at http://pubs.acs.org.

dx.doi.org/10.1021/jp2098312 | J. Phys. Chem. C 2012, 116, 2720–2727

AUTHOR INFORMATION

Corresponding Author

*E-mail: zjh@jlu.edu.cn; Fax: +86-431-85193423; Phone: +86-431-85168478.

ACKNOWLEDGMENTS

This work was supported by the National Basic Research Program of China (2012CB933802, 2012CB933803) and the National Science Foundation of China (grant nos. 91123031, 21074048, 20921003).

REFERENCES

(1) Kreibig, U.; Vollmer, M. *Optical Properties of Metal Clusters*; Springer-Verlag: Heidelberg, Germany, 1995; Vol. 25.
(2) Haes, A. J.; Haynes, C. L.; McFarland, A. D.; Schatz, G. C.; van Duyne, R. P.; Zou, S. *MRS Bull.* **2005**, *30*, 368−375.
(3) Hutter, E.; Fendler, J. H. *Adv. Mater.* **2004**, *16*, 1685−1706.
(4) Underwood, S.; Mulvaney, P. *Langmuir* **1994**, *10*, 3427−3430.
(5) (a) Kelly, K. L.; Coronado, E.; Zhao, L. L.; George, C. S. *J. Phys. Chem. B* **2003**, *107*, 668−677. (b) Wei, W.; Li, S. Z.; Millstone, J. E.; Banholzer, M. J.; Chen, X. D.; Xu, X. Y.; Schatz, G. C.; Mirkin, C. A. *Angew. Chem., Int. Ed.* **2009**, *48*, 4210−4212.
(6) (a) Zhang, X. M.; Zhang, J. H.; Wang, H.; Hao, Y. D.; Zhang, X.; Wang, T. Q.; Wang, Y. N.; Zhao, R.; Zhang, H.; Yang, B. *Nanotechnology* **2010**, *21*, 465702−465712. (b) Wei, W.; Li, S. Z.; Qin, L. D.; Xue, C.; Millstone, J. E.; Xu, X. Y.; Schatz, G. C.; Mirkin, C. A. *Nano Lett.* **2008**, *8*, 3446−3449.
(7) Kalyuzhny, G.; Vaskevich, A.; Ashkenasy, G.; Shanzer, A.; Rubinstein, I. *J. Phys. Chem. B* **2000**, *104*, 8238−8244.
(8) Kalyuzhny, G.; Schneeweiss, M. A.; Shanzer, A.; Vaskevich, A.; Rubinstein, I. *J. Am. Chem. Soc.* **2001**, *123*, 3177−3178.
(9) Yasuda, T.; Tsuji, Y.; Koshiba, M. *IEEE Photonics Technol. Lett.* **2005**, *17*, 55−57.
(10) Goettmann, F.; Moores, A.; Boissiere, C.; LeFloch, P.; Sanchez, C. *Small* **2005**, *6*, 636−639.
(11) Karakouz, T.; Vaskevich, A.; Rubinstein, I. *J. Phys. Chem. B* **2008**, *112*, 14530−14538.
(12) Stewart, M. E.; Anderton, C. R.; Thompson, L. B.; Maria, J.; Gray, S. K.; Rogers, J. A.; Nuzzo, R. G. *Chem. Rev.* **2008**, *108*, 494−521.
(13) Li, Y. F.; Zhang, J. H.; Wang, T. Q.; Zhu, S. J.; Yu, H. J.; Fang, L. P.; Wang, Z. H.; Cui, L. Y.; Yang, B. *J. Phys. Chem. C* **2010**, *114*, 19908−19912.
(14) Haes, A. J.; Hall, W. P.; Chang, L.; Klein, W. L.; Van Duyne, R. P. *Nano Lett.* **2004**, *4*, 1029−1034.
(15) Jonsson, M. P.; Jonsson, P.; Dahlin, A. B.; Hook, F. *Nano Lett.* **2007**, *7*, 3462−3468.
(16) Hutter, E.; Pileni, M. P. *J. Phys. Chem. B.* **2003**, *107*, 6497−6499.
(17) Hiep, H. M.; Endo, T.; Saito, M.; Chikae, M.; Kim, D. K.; Yamamura, S.; Takamura, Y.; Tamiya, E. *Anal. Chem.* **2008**, *80*, 1859−1864.
(18) Nath, N.; Chilkoti, A. *Anal. Chem.* **2004**, *76*, 5370−5378.
(19) Marinakos, S. M.; Chen, S.; Chilkoti, A. *Anal. Chem.* **2007**, *79*, 5278−5283.
(20) Bendikov, T. A.; Rabinkov, A.; Karakouz, T.; Vaskevich, A.; Rubinstein, I. *Anal. Chem.* **2008**, *80*, 7487−7498.
(21) Hsiao, V. K. S.; Kirkey, W. D.; Chen, F.; Cartwright, A. N.; Prasad, P. N.; Bunning, T. J. *Adv. Mater.* **2005**, *17*, 2211−2214.
(22) Urbas, A.; Klosterman, J.; Tondiglia, V.; Natarajan, L.; Sutherland, R.; Tsutsumi, O.; Ikeda, T.; Bunning, T. *Adv. Mater.* **2004**, *16*, 1453−1456.
(23) Hsiao, V. K. S.; Li, Z.; Chen, Z.; Peng, P. C.; Tang, J. Y. *Opt. Express.* **2009**, *17*, 19988−19995.
(24) Hsiao, V. K. S.; Zheng, Y. B.; Juluri, B. K.; Huang, T. J. *Adv. Mater.* **2008**, *20*, 3528−3532.
(25) Hu, W.; Zhao, H. Y.; Song, L.; Yang, Z.; Cao, H.; Cheng, Z. H.; Liu, Q.; Yang, H. *Adv. Mater.* **2010**, *22*, 468−472.
(26) Sutherland, R. L.; Tondiglia, V. P.; Natarajan, L. V.; Bunning, T. J.; Adams, W. W. *Appl. Phys. Lett.* **1994**, *64*, 1074−1076.
(27) Humar, M.; Ravnik, M.; Pajk, S.; Musevic, I. *Nat. Photonics* **2009**, *3*, 595−600.
(28) Choi, S. S.; Morris, S. M.; Huck, W. T. S.; Coles, H. J. *Adv. Mater.* **2009**, *21*, 3915−3918.
(29) Puzzo, D. P.; Arsenault, A. C.; Manners, I.; Ozin, G. A. *Angew. Chem., Int. Ed.* **2009**, *48*, 943−947.
(30) Yeh, P.; Gu, C. *Optics of Liquid Crystal Displays*; John Wiley and Sons: New York, 1999.
(31) Kossyrev, P.; Sousa, M. E.; Crawford, G. *Adv. Funct. Mater.* **2004**, *14*, 1227−1232.
(32) Escuti, M. J.; Qi, J.; Crawford, G. P. *Opt. Lett.* **2003**, *28*, 522−524.
(33) Bowley, C. C.; Kossyrev, P. A.; Crawford, G. P.; Faris, S. *Appl. Phys. Lett.* **2001**, *79*, 9−11.
(34) Guzman, O.; Kim, E. B.; Grollau, S.; Abbott, N. L.; Pablo, J. J. *Phys. Rev. Lett.* **2003**, *91*, 235507−235510.
(35) Kim, J. K.; VanLe, K.; Dhara, S.; Araoka, F.; Ishikawa, K.; Takezoeb, H. *J. Appl. Phys.* **2010**, *107*, 123108−123111.
(36) Kossyrev, P. A.; Yin, A.; Cloutier, S. G.; Cardimona, D. A.; Huang, D. H.; Alsing, P. M.; Xu, J. M. *Nano Lett.* **2005**, *5*, 1978−1981.
(37) Miyazaki, T.; Hasegawa, R.; Yamaguchi, H.; Oh-oka, H.; Nagato, H.; Amemiya, I.; Uchikoga, S. *J. Phys. Chem. C* **2009**, *113*, 8484−8490.
(38) Chu, K. C.; Chao, C. Y.; Chen, Y. F.; Wu, Y. C.; Chen, C. C. *Appl. Phys. Lett.* **2006**, *89*, 103107−103109.
(39) (a) Kubo, S.; Gu, Z. Z.; Takahashi, K.; Fujishima, A.; Segawa, H.; Sato, O. *Chem. Mater.* **2005**, *17*, 2298−2309. (b) Gu, Z. Z.; Iyoda, T.; Fujishima, A.; Sato, O. *Adv. Mater.* **2001**, *13*, 1295−1298. (c) Xie, Z. Y.; Sun, L. G.; Han, G. Z.; Gu, Z. Z. *Adv. Mater.* **2008**, *20*, 3601−3604.
(40) Koenig, G. M.; Gettelfinger, B. T.; Pablo, J. J.; Abbott, N. L. *Nano Lett.* **2008**, *8*, 2362−2368.
(41) Khatua, S.; Manna, P.; Chang, W. S.; Tcherniak, A.; Friedlander, E.; Zubarev, E. R.; Link, S. *J. Phys. Chem. C* **2010**, *114*, 7251−7257.
(42) Yoshida, H.; Kawamoto, K.; Kubo, H.; Tsuda, T.; Fujii, A.; Kuwabata, S.; Ozaki, M. *Adv. Mater.* **2010**, *22*, 622−626.
(43) Müller, J.; Sönnichsen, C.; Poschinger, H.; Plessen, G.; Klar, T. A.; Feldmann, J. *Appl. Phys. Lett.* **2002**, *81*, 171−173.
(44) Liu, Q. K.; Cui, Y. X.; Gardner, D.; Li, X.; He, S.; Smalyukh, I. I. *Nano Lett.* **2010**, *10*, 1347−1353.
(45) Dridi, M.; Vial, A. *J. Phys. Chem. C* **2010**, *114*, 9541−9545.
(46) Koenig, G. M.; Meli, M. V.; Park, J. S.; Pablo, J. J.; Abbott, N. L. *Chem. Mater.* **2007**, *19*, 1053−1061.
(47) Koenig, G. M.; Ong, R.; Cortes, A. D.; Moreno-Razo, J. A.; Pablo, J. J.; Abbott, N. L. *Nano Lett.* **2009**, *9*, 2794−2801.
(48) Koenig, G. M.; Gettelfinger, B. T.; Pablo, J. J.; Abbott, N. L. *Nano Lett.* **2008**, *8*, 2362−2368.
(49) Stark, H. *Phys. Rev. E* **2002**, *66*, 041705−041508.
(50) Borstnik, A.; Stark, H.; Zumer, S. *Phys. Rev. E* **1999**, *60*, 4210−4218.
(51) Borstnik, A.; Stark, H.; Zumer, S. *Phys. Rev. E* **2000**, *61*, 2831−2839.
(52) Kuksenok, O. V.; Ruhwandl, R. W.; Shiyanovskii, S. V.; Terentjev, E. M. *Phys. Rev. E* **1996**, *54*, 5198−5023.
(53) Ruhwandl, R. W.; Terentjev, E. M. *Phys. Rev. E* **1996**, *54*, 5204−5210.
(54) Ruhwandl, R. W.; Terentjev, E. M. *Phys. Rev. E* **1997**, *56*, 5561−5565.
(55) Fukuda, J. I.; Stark, H.; Yoneya, M.; Yokoyama, H. *Phys. Rev. E* **2004**, *69*, 041706−041715.
(56) Fukuda, J. I.; Stark, H.; Yokoyama, H. *Phys. Rev. E* **2005**, *72*, 021701−021710.
(57) Stark, H.; Fukuda, J. I.; Yokoyama, H. *Phys. Rev. Lett.* **2004**, *92*, 205502−205505.
(58) Jasieniak, J.; Sada, C.; Chiasera, A.; Ferrari, M.; Martucci, A.; Mulvaney, P. *Adv. Funct. Mater.* **2008**, *18*, 3772−3779.
(59) White, D. L.; Taylor, G. N. *J. Appl. Phys.* **1974**, *45*, 4718−4723.
(60) Frens, G. *Nature Phys. Sci.* **1973**, *241*, 20−22.

(61) Reincke, F.; Hickey, S. G.; Kegel, W. K.; Vanmaekelbergh, D. *Angew. Chem. Int. Ed* **2004**, *43*, 458−462.
(62) Park, P. Y.; Park, S. *Chem. Mater.* **2008**, *20*, 2388−2393.
(63) Park, Y. K.; Yoo, S. K.; Park, S. *Langmuir* **2007**, *23*, 10505−10510.
(64) Miller, M. M.; Lazarides, A. A. *J. Phys. Chem. B* **2005**, *109*, 21556−21565.
(65) Lee, K. S.; El-Sayed, M. A. *J. Phys. Chem. B* **2006**, *110*, 19220−19225.
(66) Karakouz, T.; Holder, D.; Goomanovsky, M.; Vaskevich, A.; Rubinstein, I. *Chem. Mater.* **2009**, *21*, 5875−5885.
(67) Haes, A. J.; Van Duyne, R. P. *Expert Rev. Mol. Diagn.* **2004**, *4*, 527−537.
(68) Ozaki, M.; Shimoda, Y.; Kasano, M.; Yoshino, K. *Adv. Mater.* **2002**, *14*, 514−518.